CPOD 2017,
Stony Brook,
7-11 VIII 2017

Kaon spectra in Ar+Sc collisions at 30*A*, 40*A* and 75*A* GeV/*c*

Maciej Lewicki
mlewicki@ift.uni.wroc.pl

for the
NA61/SHINE
Collaboration

Uniwersytet Wrocławski

Outline

1. NA61/SHINE strong interaction programme.
2. Particle identification through dE/dx vs p information.
3. Preliminary results on kaon production in ^{40}Ar+^{45}Sc collisions at three beam momenta:

   30*A*, **40***A* and **75***A* GeV/c $\rightarrow$ $\sqrt{s_{NN}} = 7.6,\ 8.8,\ 11.9$ GeV.

   Selected 5% most "violent" ($\approx$ central) events.
4. Comparison with world data, with special attention to **system size dependence**.

Outline

Preliminary results on **kaons** (K^+ and K^-) produced in strong and electromagnetic processes in primary interactions:

- Double differential spectra in y and p_T.
- p_T distributions.
- Rapidity distributions.
- Rapidity spectra interpolation. Mean multiplicities.

Results for Ar+Sc will be compared with:

- Be+Be – NA61/SHINE preliminary data.
- p+p – NA61/SHINE data.

  [CERN-EP-2017-066]
- Pb+Pb, C+C, Si+Si – NA49 data.

  [Phys.Rev. C77, 024903 (2008)], [Phys.Rev. C66 (2002) 054902], [Phys.Rev. C86 (2012) 054903]

Section 1

NA61/SHINE strong interaction programme

NA61/SHINE's strong interaction programme

Two-dimensional scan in collision energy and system size probes the phase diagram of strongly interacting matter:

- Search for the **critical point**.
- Study of the **onset of deconfinement**.

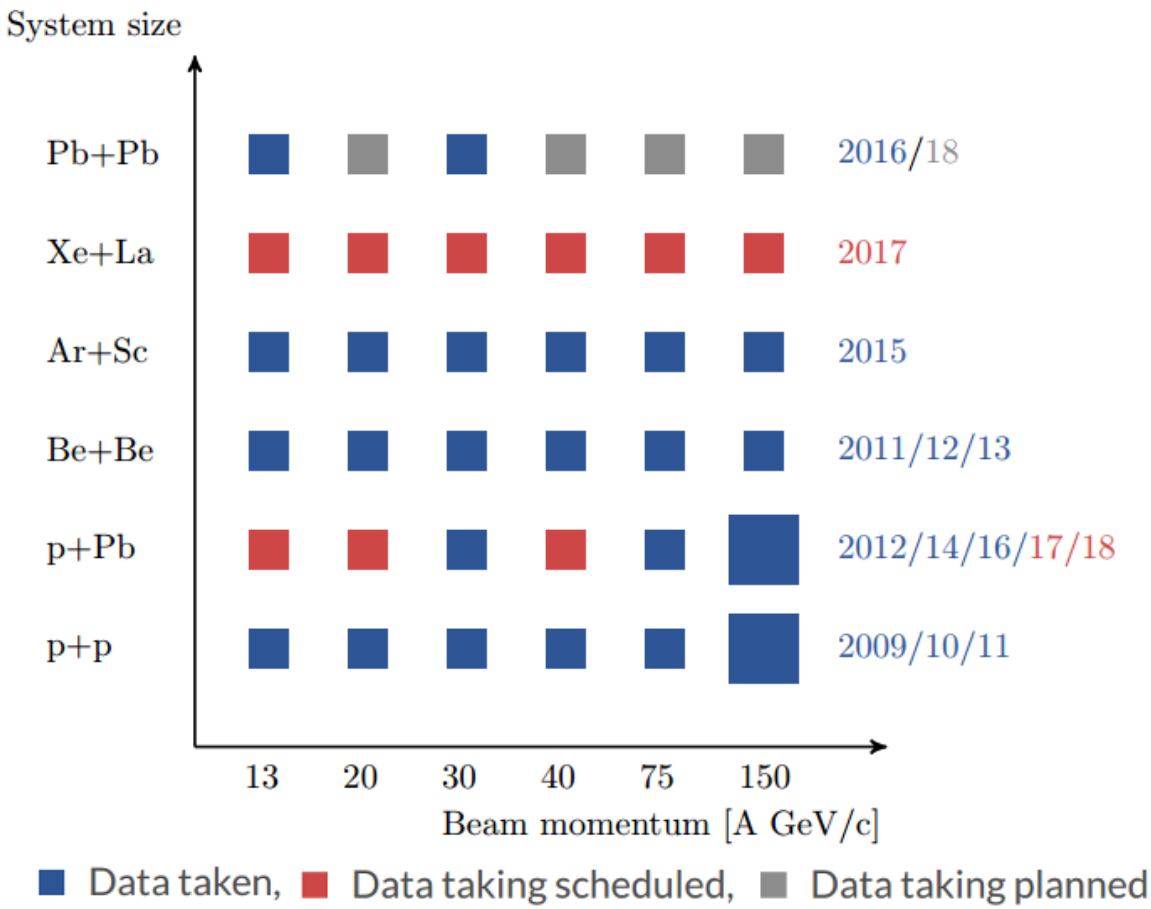

Section 2

dE/dx analysis method

$\langle dE/dx \rangle$ VS p_{tot} DISTRIBUTION

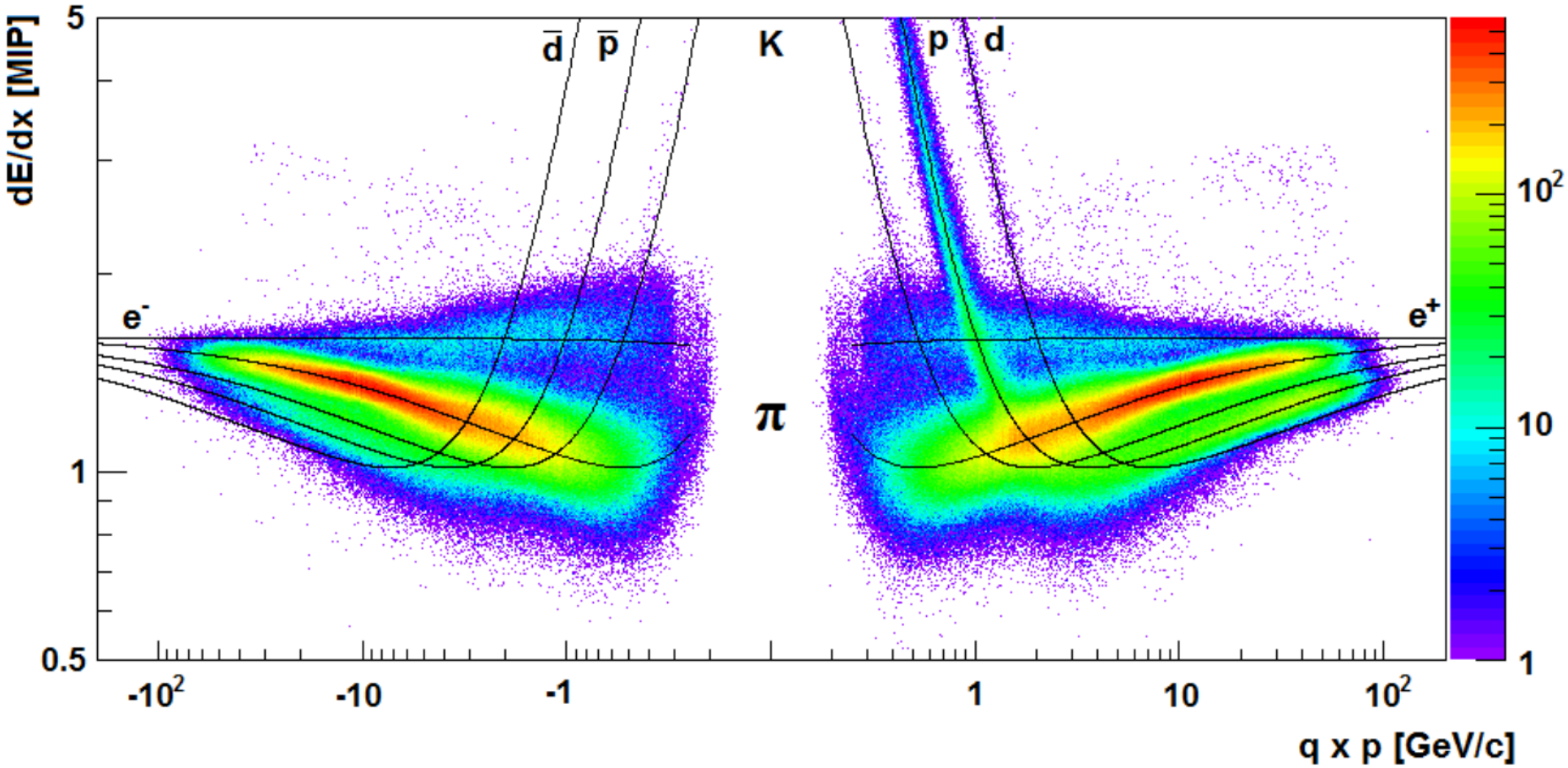

Distribution of energy loss vs total momentum in NA61/SHINE's TPCs.

Bin by bin spectra fitting

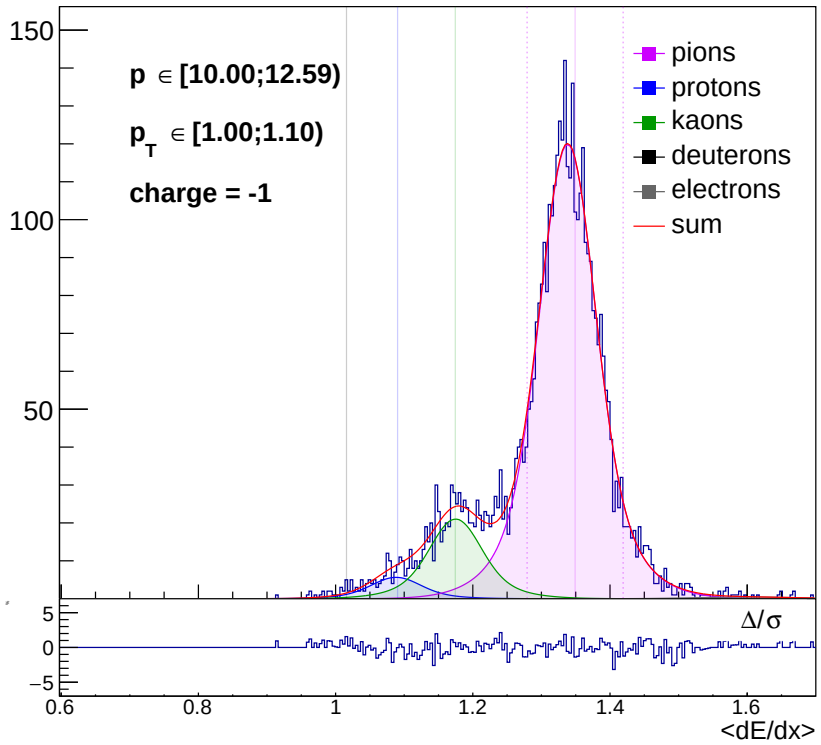

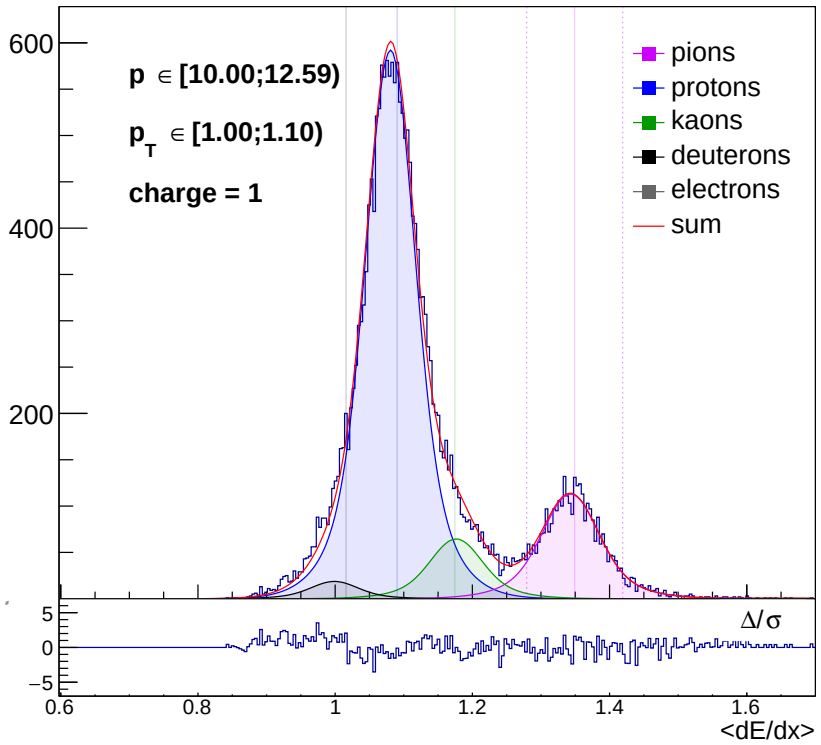

Example distributions and particle yield fits in a single bin of 30*A* GeV/*c* data.

Fits were performed in 13 logarithmic bins in $p \in [5, 100]$ GeV/*c* and 20 linear bins in $p_T \in [0.0, 2.0]$ GeV/*c*.

Extracting $y : p_T$ spectra

Track by track probability calculation:

$$P_i\left(p, p_T, {}^{dE}/_{dx}\right) = \frac{f_i\left(p, p_T, {}^{dE}/_{dx}\right)}{\sum_i f_i\left(p, p_T, {}^{dE}/_{dx}\right)}$$

The number of particles of type i in a given bin:

$$n_{i \in \{\pi^-, \pi^+, K^-, K^+, p, \bar{p}\}} = \sum_{j=1}^{n} P_i$$

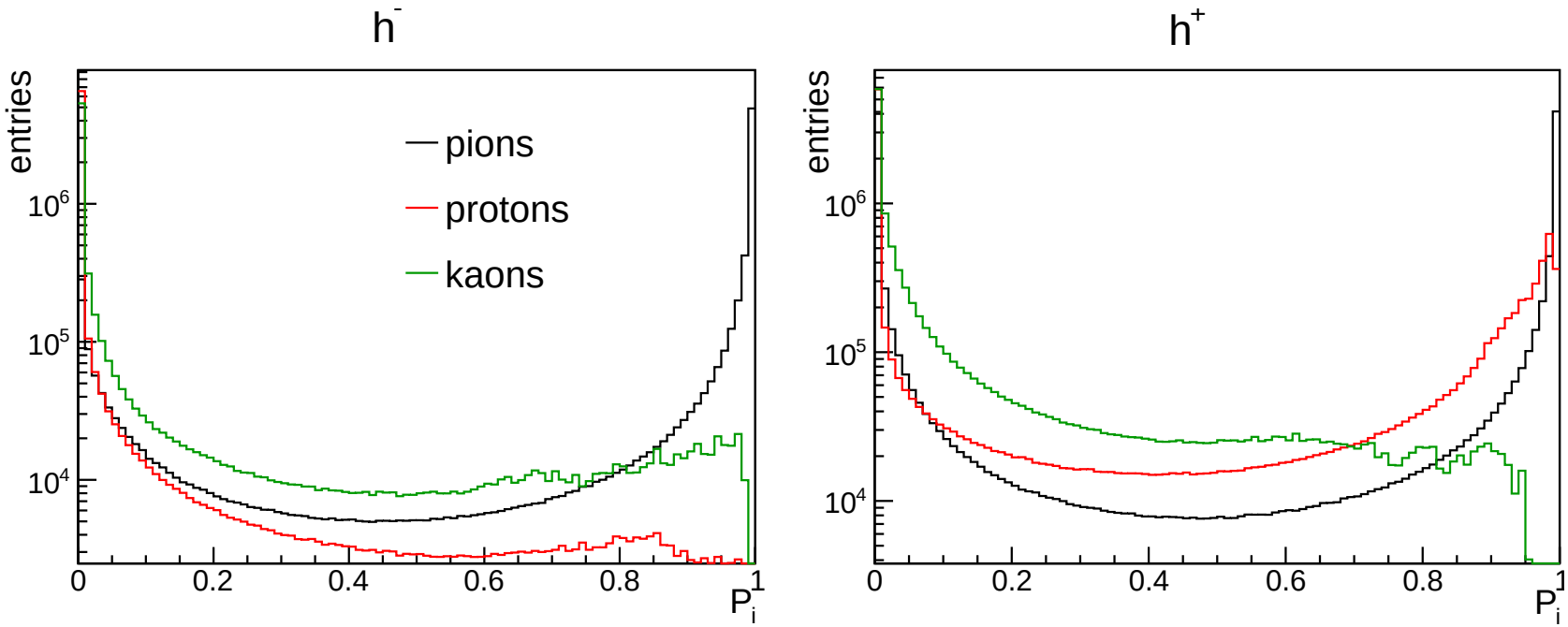

Sample distribution of probabilities obtained for 75A GeV/c

Event selection in Ar+Sc collisions

Centrality classes – Projectile Spectator Detector

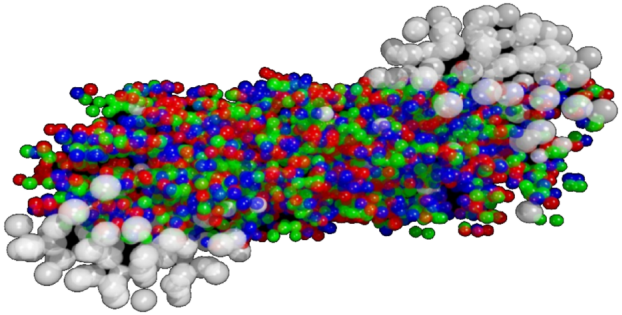

→

- The PSD is located most downstream on the beam line and measures the projectile spectator energy E_F of the non-interacting nucleons of the beam nucleus.
- The energy measured by the PSD is used to select events classes corresponding to the collision centrality.

Note on corrections and uncertainties

Model Corrections

- Monte Carlo used for corrections: EPOS1.99 model (version CRMC 1.5.3), GEANT3.2.
- The centrality classes selected by the number of forward spectators.

Uncertainties

- Data points are drawn with statistical uncertainties only. There are two sources:
  - Data uncertainties.
  - MC corrections uncertainties (insignificant).
- The systematic uncertainties are still under study
  (rapidity interpolation uncertainties are discussed later).

Section 3

p_T vs y spectra of kaons

30A GeV/c

p_T vs y

Preliminary double differential spectra:

$$\frac{dn^2}{dy\,dp_T}$$

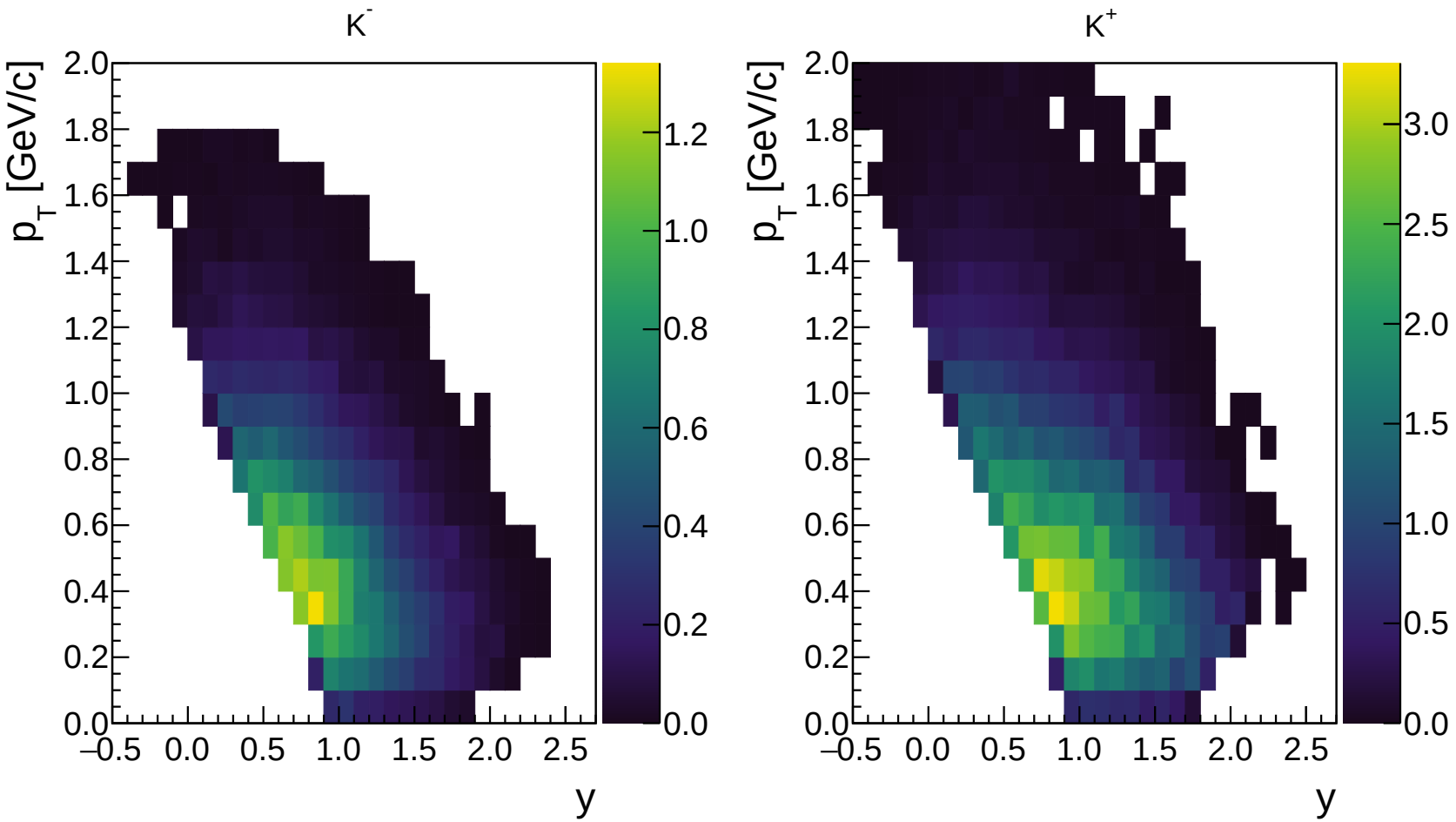

40A GeV/c

p_T vs y

Preliminary double differential spectra:

$$\frac{dn^2}{dy\,dp_T}$$

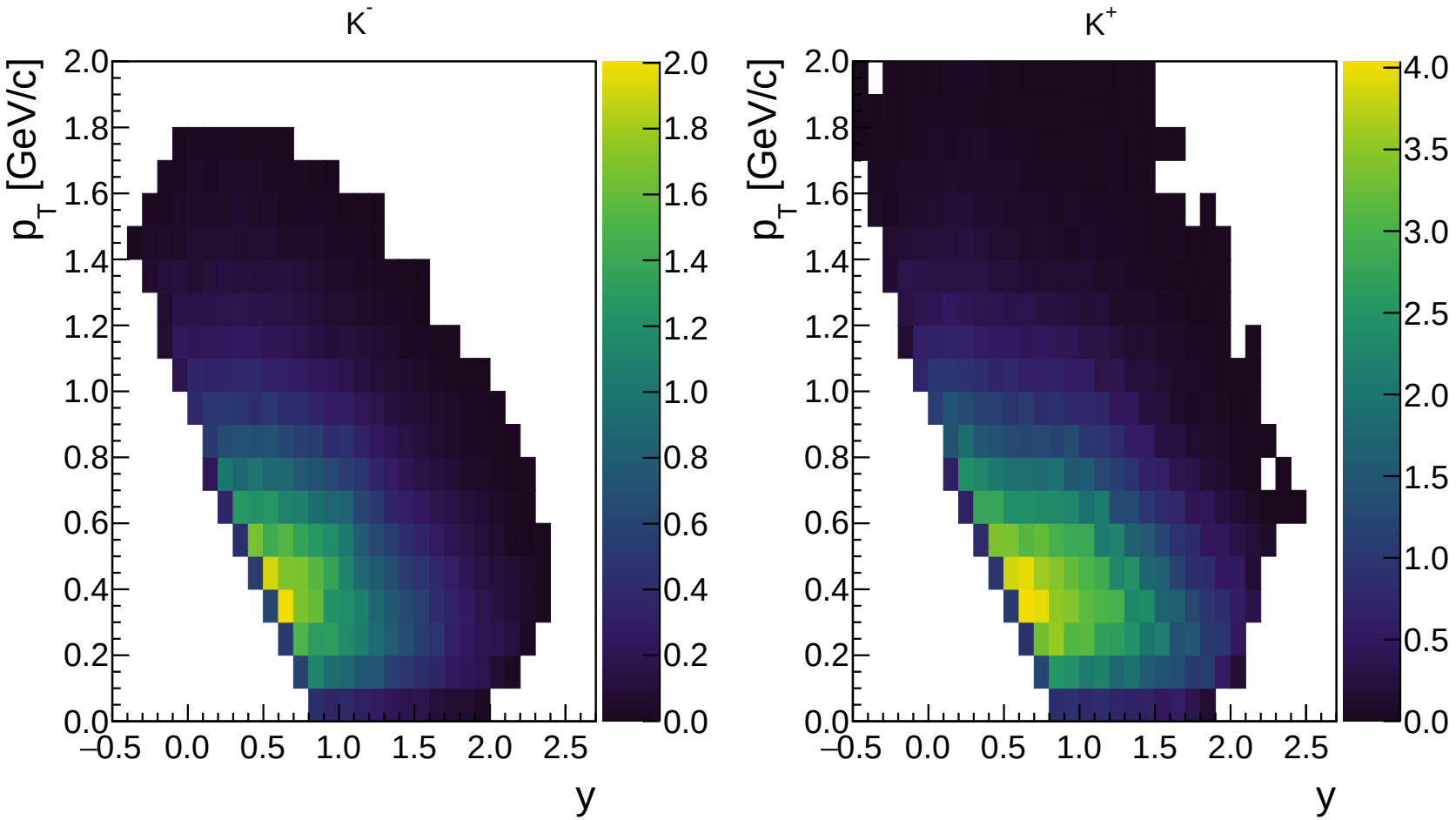

75A GeV/c

p_T vs y

Preliminary double differential spectra:

$$\frac{dn^2}{dy\,dp_T}$$

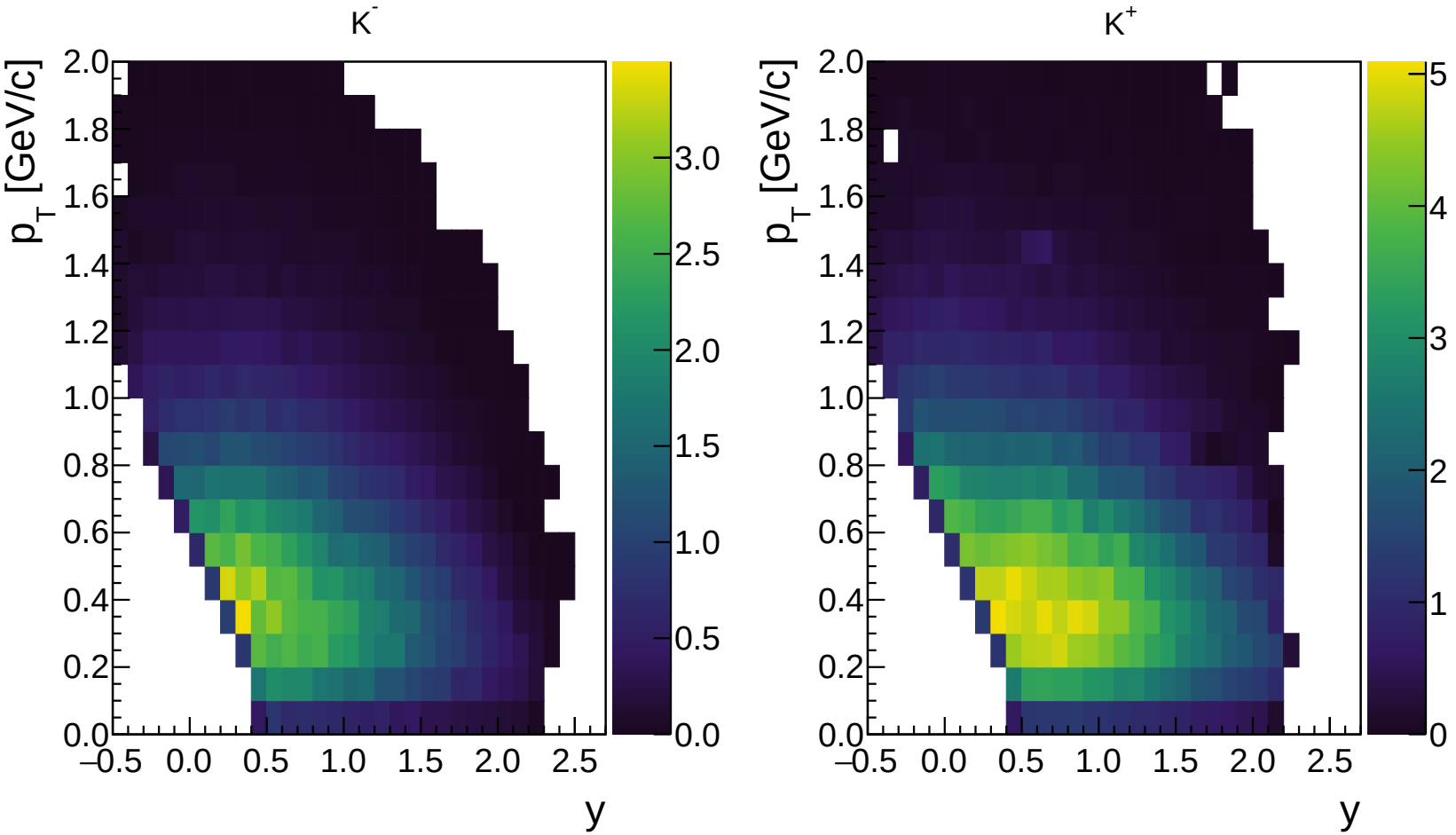

Section 4

Transverse momentum distribution of kaons

30A GeV/c – p_T DISTRIBUTIONS

Ar+Sc → K^-+X at 30A GeV/c

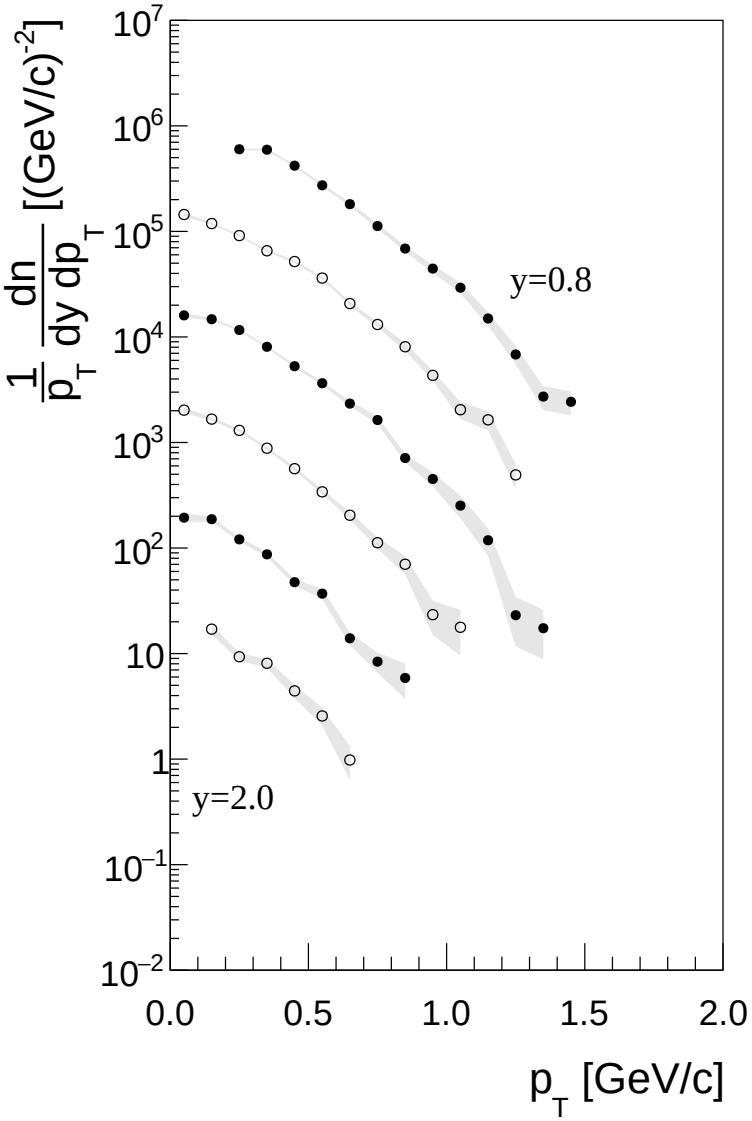

Ar+Sc → K^++X at 30A GeV/c

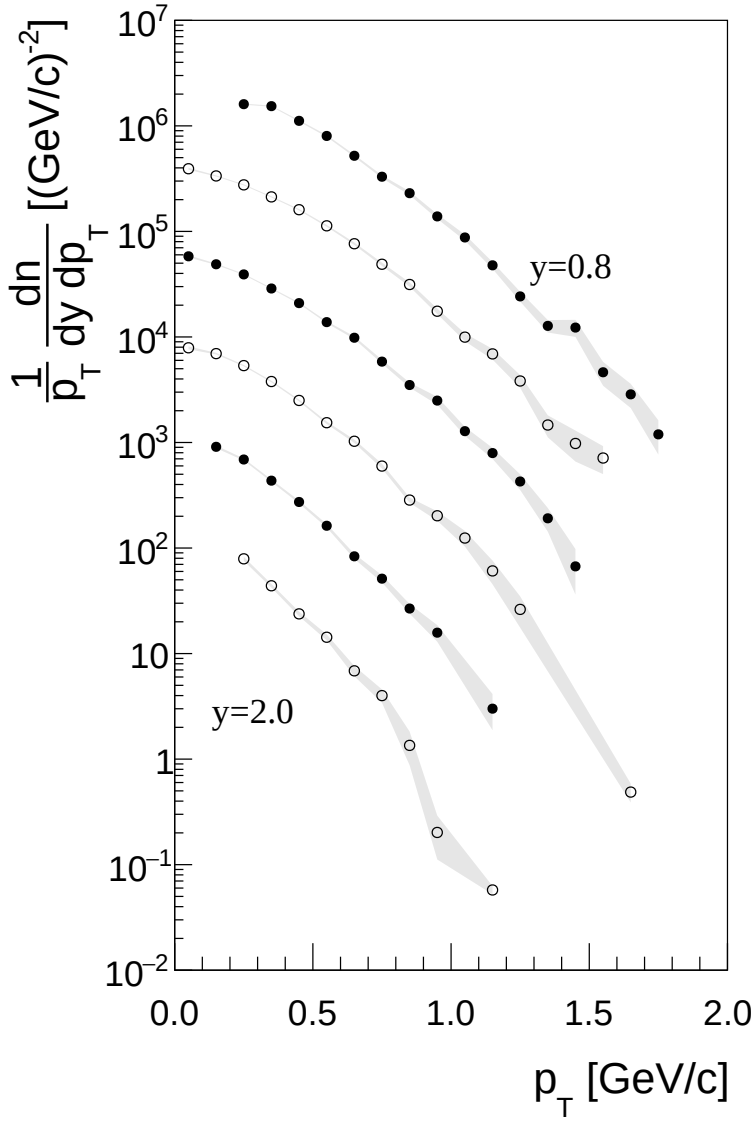

40A GeV/c – p_T DISTRIBUTIONS

Ar+Sc → K^-+X at 40A GeV/c

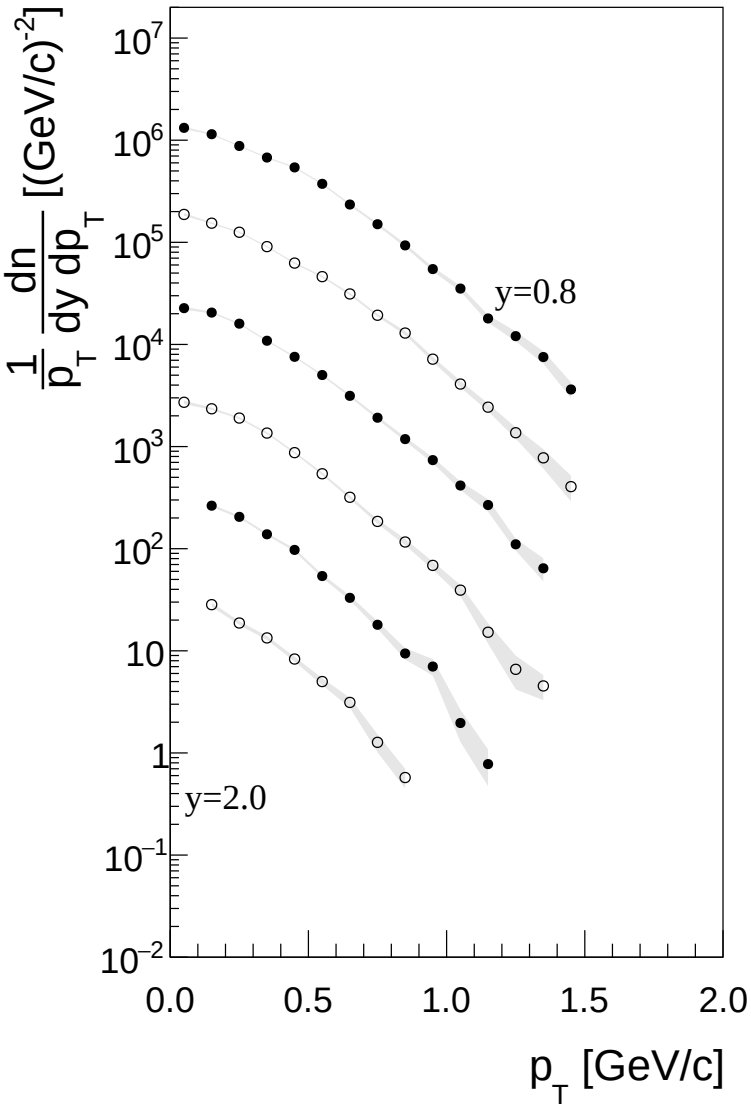

Ar+Sc → K^++X at 40A GeV/c

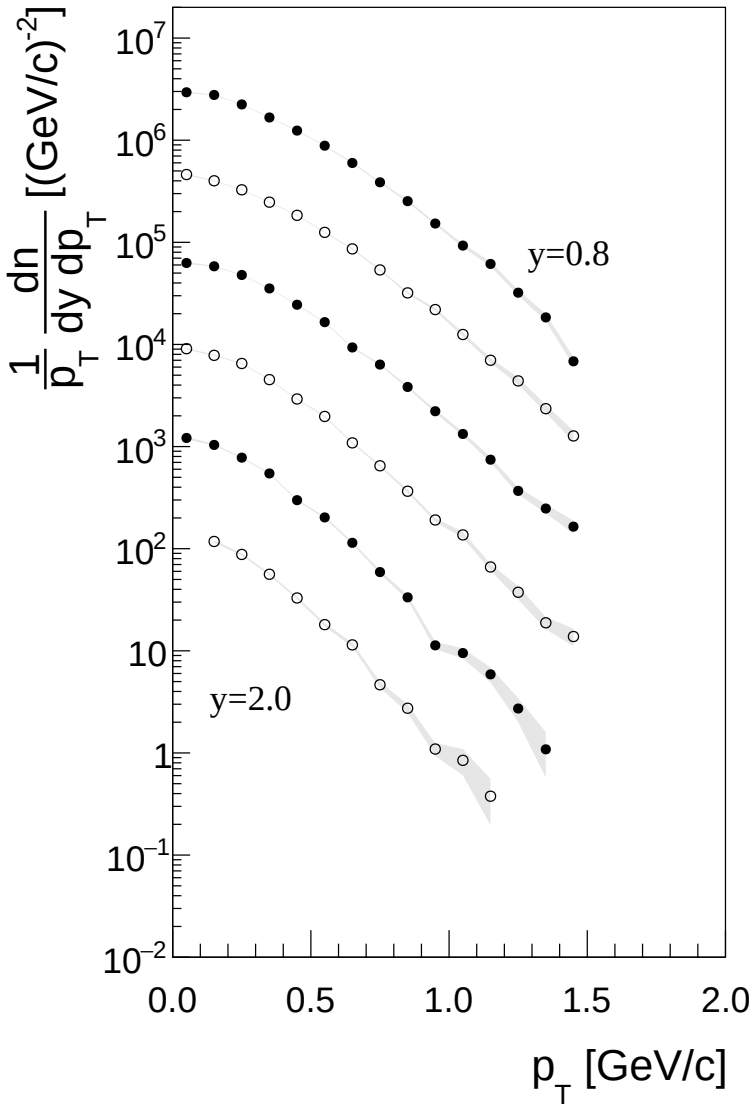

75A GeV/c – p_T DISTRIBUTIONS

Ar+Sc → K^-+X at 75A GeV/c

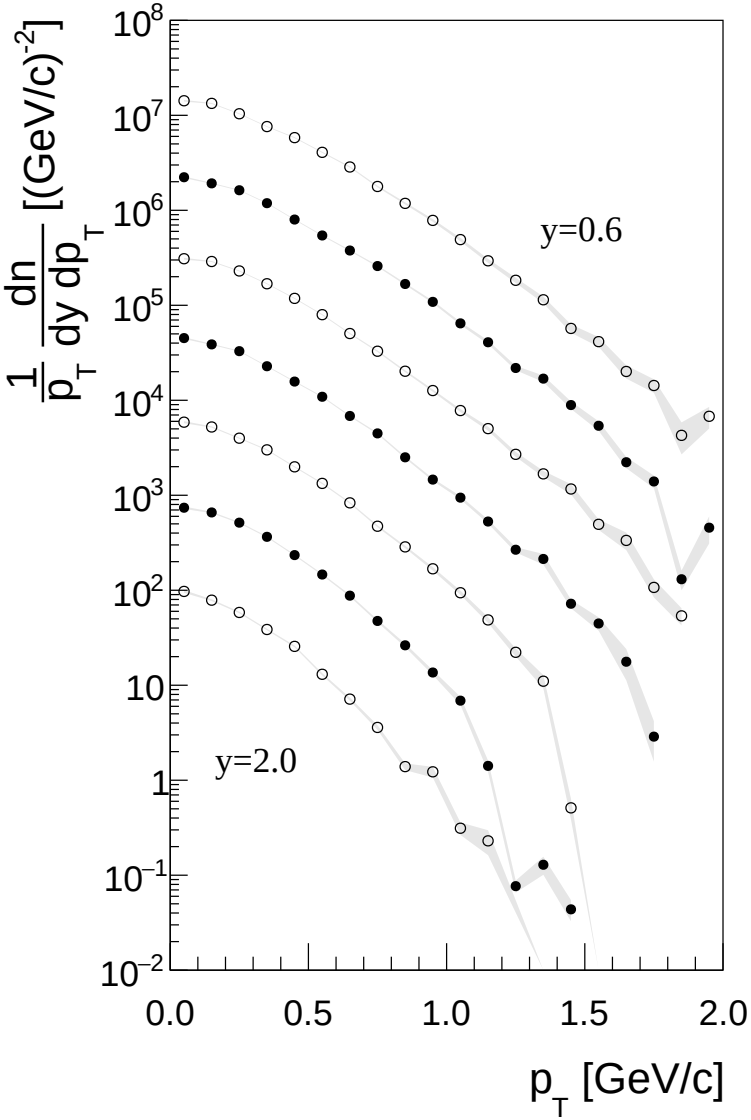

Ar+Sc → K^++X at 75A GeV/c

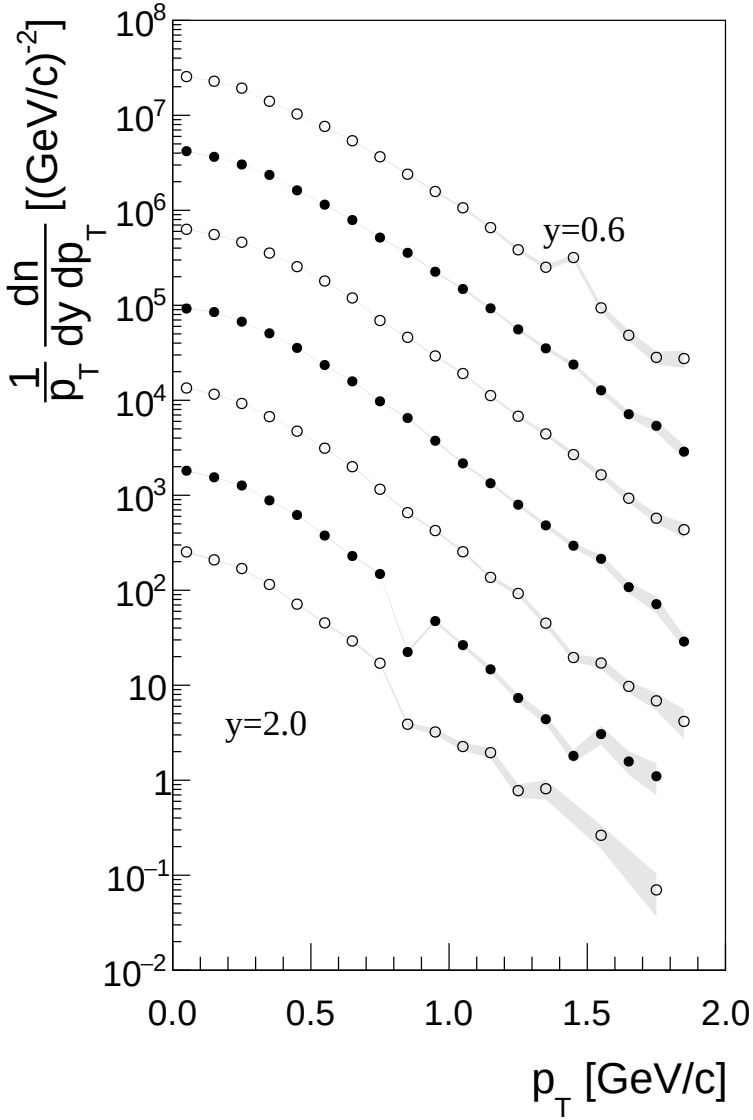

Extrapolation in p_T

- In order to obtain dn/dy yields, the data is extrapolated in p_T to account for unmeasured regions.
- Exponential dependence in p_T is assumed:

$$\frac{1}{p_T}\frac{d^2}{dp_T\,dy} = \frac{dn/dy}{T\cdot(m_K+T)}\cdot e^{-(m_T-m_K)/T}$$

- The function integral outside the acceptance region is added to the measured data points (typically of the order of 1%).

Inverse slope parameter T

Extrapolation of Ar+Sc points to $T(y \approx 0)$ falls close to Pb+Pb, while smaller systems are placed significantly lower.

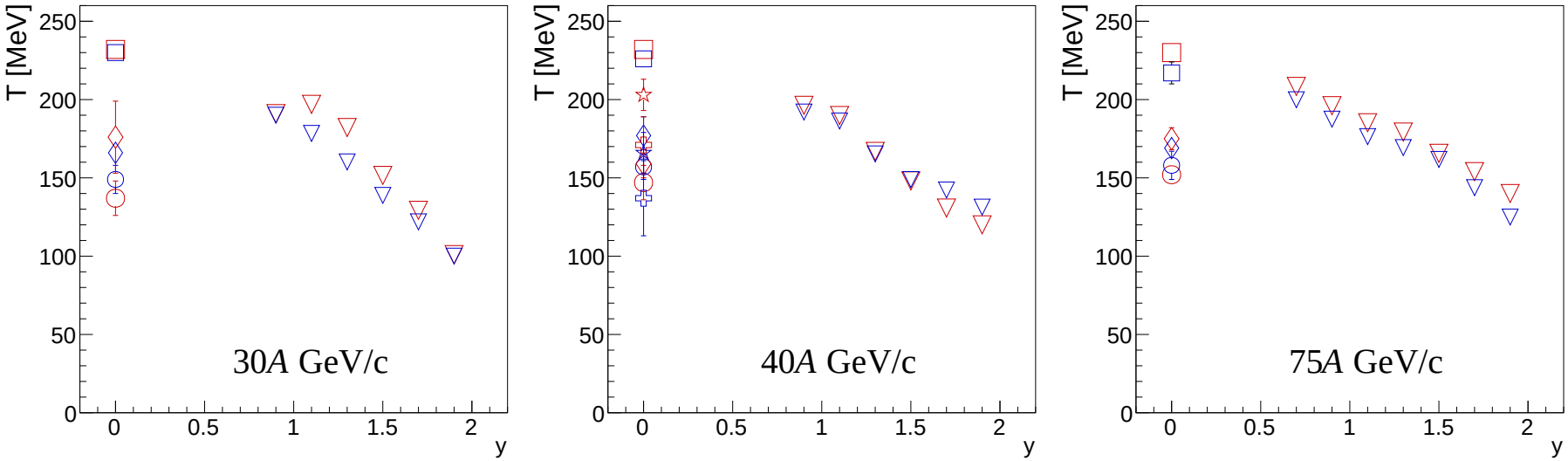

NA61/SHINE

Ar+Sc	Be+Be	p+p
▽ K^+	◊ K^+	○ K^+
▽ K^-	◊ K^-	○ K^-

Preliminary

NA49

Pb+Pb	C+C	Si+Si
□ K^+	✜ K^+	☆ K^+
□ K^-	✜ K^-	☆ K^-

Section 5

Rapidity distribution of kaons

Fitting rapidity distribution

Two symmetrically placed gaussians are used to construct the fitting function:

$$f_{fit}(y) = \frac{A}{\sigma_0\sqrt{2\pi}} \exp\left(-\frac{(y-y_0)^2}{2\sigma_0^2}\right) + \frac{A}{\sigma_0\sqrt{2\pi}} \exp\left(-\frac{(y+y_0)^2}{2\sigma_0^2}\right)$$

Shape parameters: y_0 and σ are fixed to values obtained in NA49's Pb+Pb.

The amplitude A is the only free parameter.

Varying the shape parameters provides an estimate of a systematic error.

Rapidity Distribution

30*A* GeV/*c*

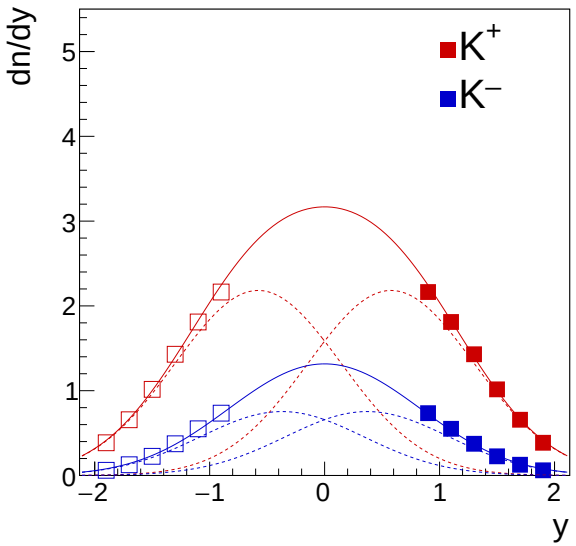

40*A* GeV/*c*

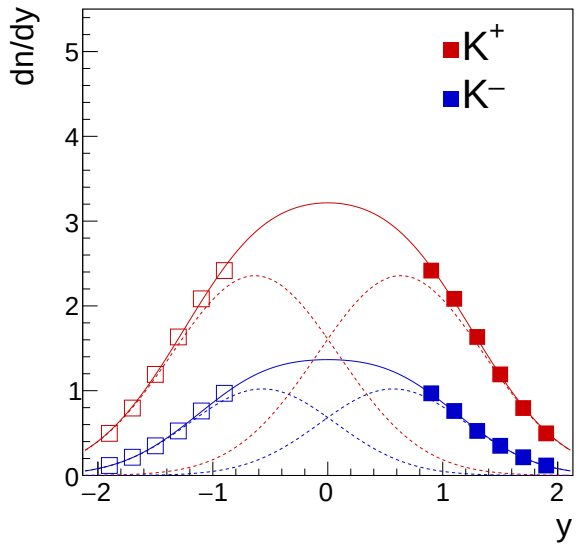

75*A* GeV/*c*

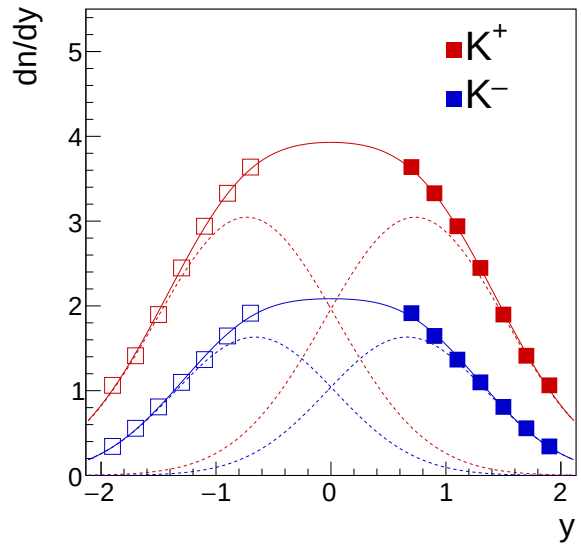

Pb+Pb spectra shape fits **Ar+Sc** data surprisingly well.

Measurements of *tof* will add data in $y \approx 0$ region in the near future.

Section 6

Mean multiplicities with comparison to other systems

$\langle K^+ \rangle$ / $\langle \pi^+ \rangle$

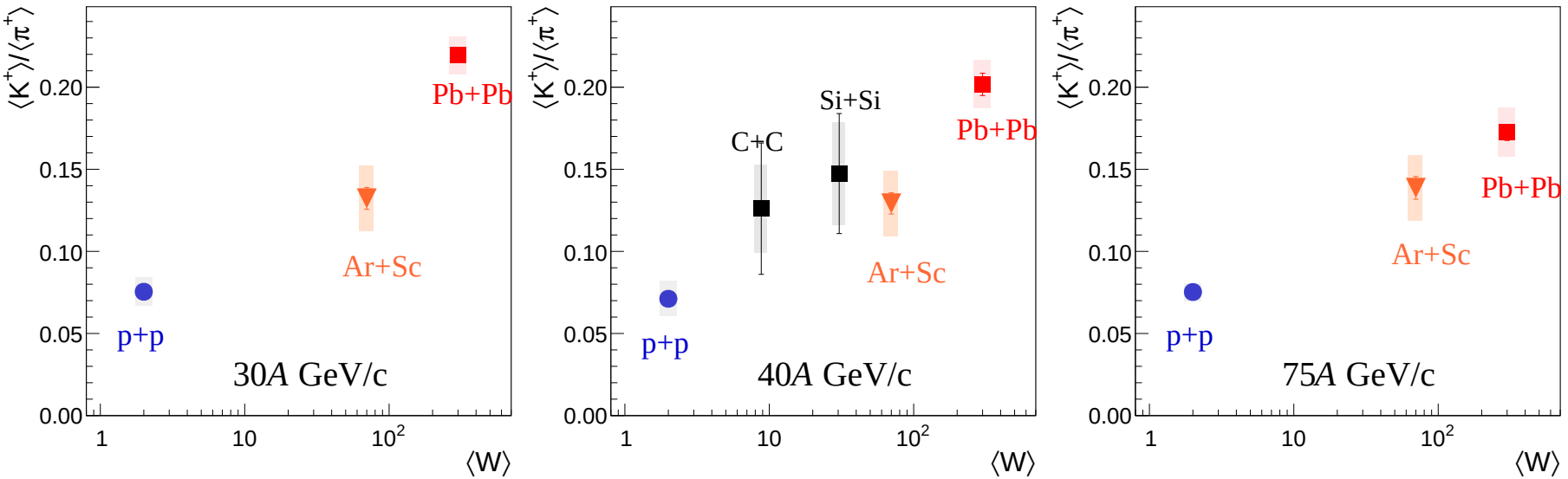

$\langle K^+ \rangle$ / $\langle \pi^+ \rangle$ ratio for 5% most violent **Ar+Sc** between **p+p** and **Pb+Pb**.

$\langle K^- \rangle$ / $\langle \pi^- \rangle$

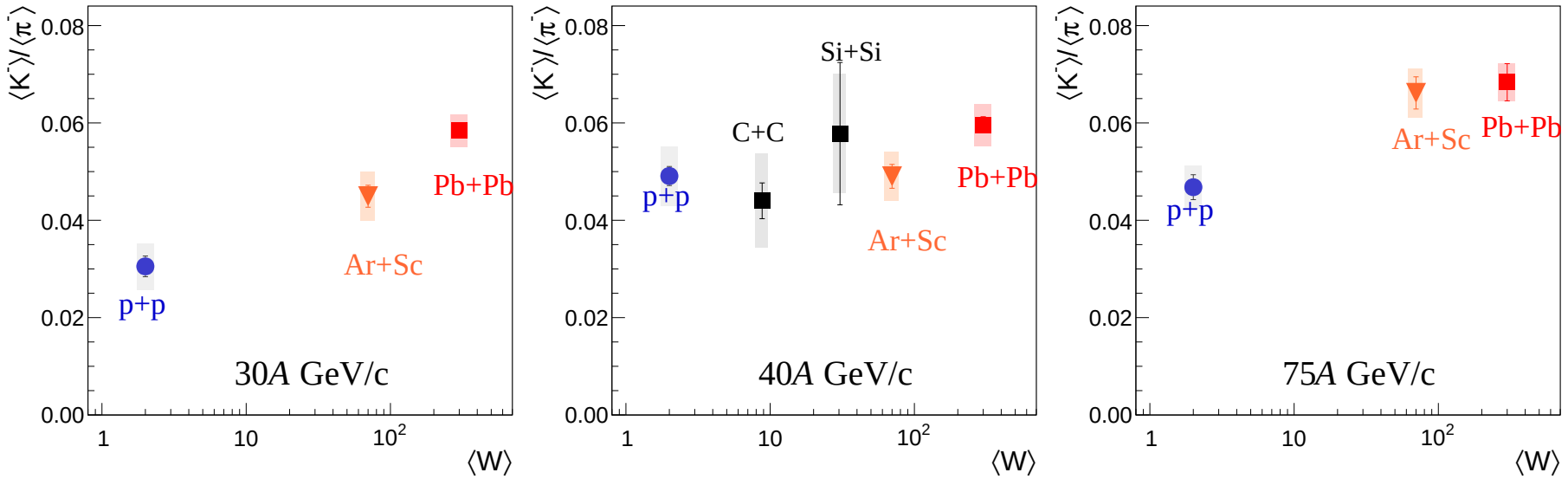

$\langle K^- \rangle$ / $\langle \pi^- \rangle$ ratio for 5% most violent **Ar+Sc** shows a monotonic behavior with increasing collision energy.

Ar+Sc is in between **p+p** and **Pb+Pb** for all energies.

$\langle K^+ \rangle$ / $\langle K^- \rangle$

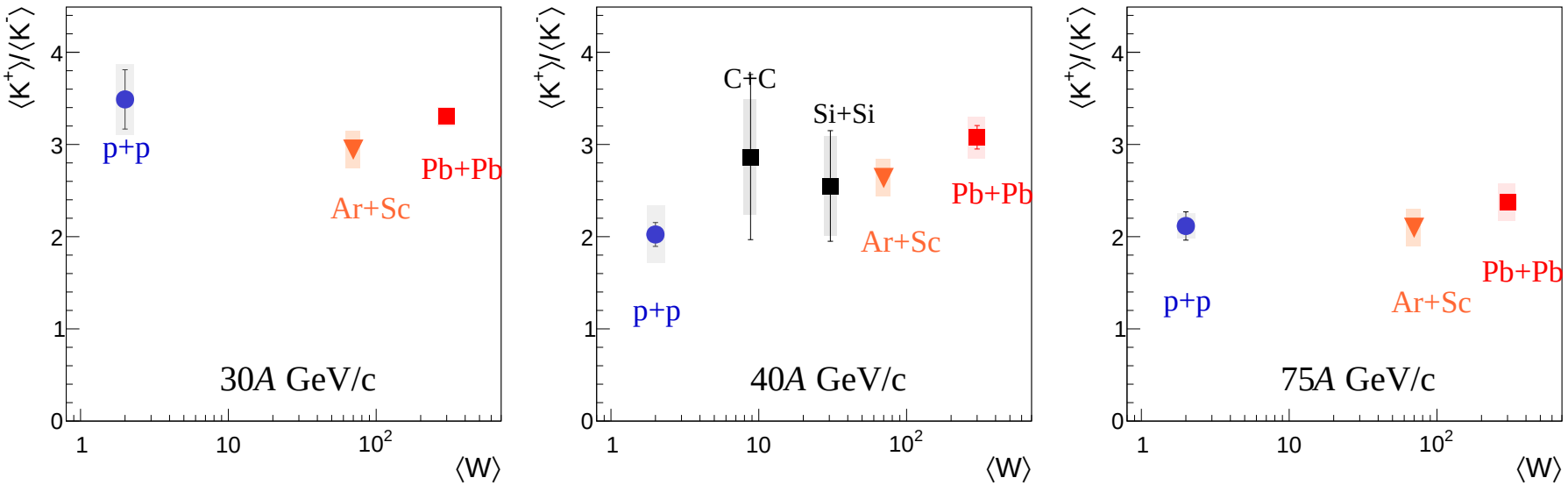

No clear system size dependence. Monotonic decrease with collision energy.

Energy dependence of $\langle K^+ \rangle / \langle \pi^+ \rangle$

"the horn" plot

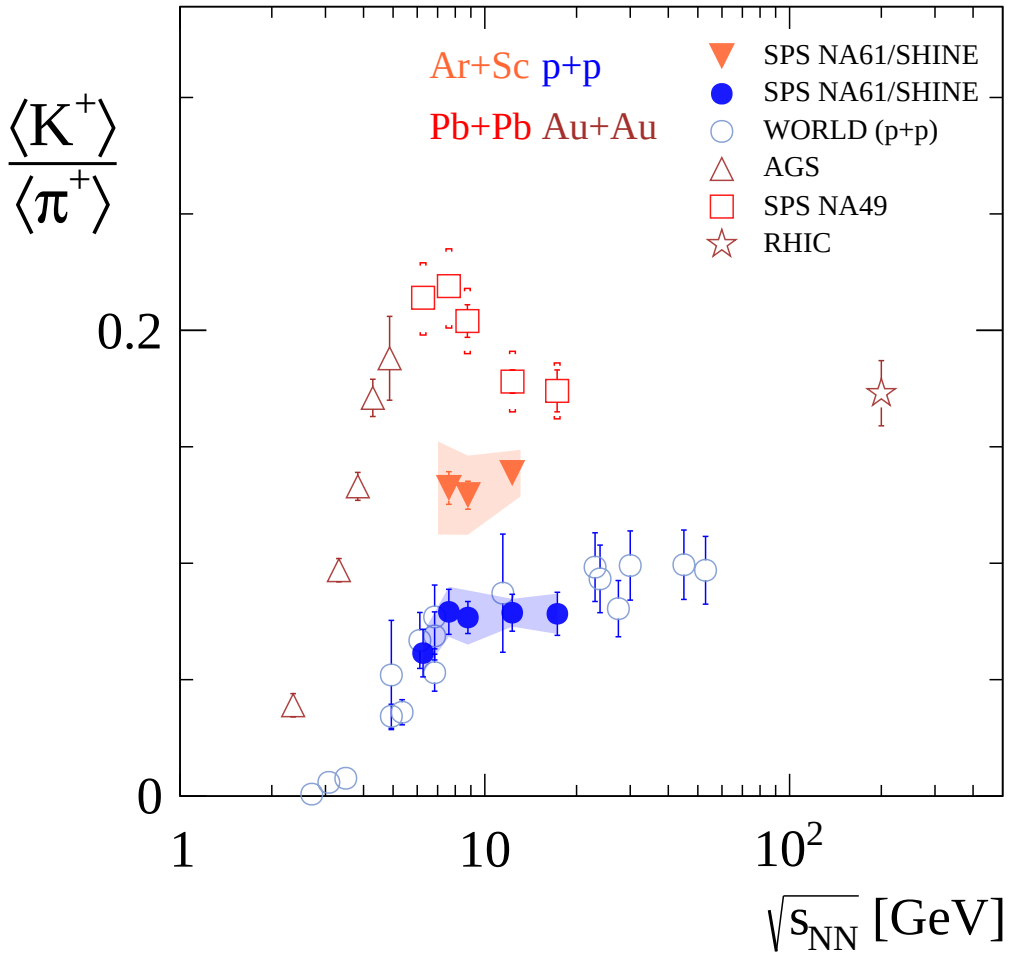

No clear energy dependence, no horn structure visible.

Ratio placed between **p+p** and **Pb+Pb**.

Section 7

Conclusions

Conclusions

Preliminary results on **kaon** production properties in 5% most violent **Ar+Sc** collisions at three beam momenta (30*A*, 40*A*, 75*A* GeV/*c*) were presented.

- p_T spectra of K^+ and K^- in the forward rapidity region were presented.
- Measured inverse slope parameter T shows trend, which extrapolates to mid-rapidity values for central **Pb+Pb**.
- Measured rapidity spectra are consistent with **Pb+Pb** spectra (shape-wise).
- $\langle K^+ \rangle$ to $\langle \pi^+ \rangle$ ratio for **Ar+Sc** between **p+p** and **Pb+Pb**.
  No horn structure visible.
- $\langle K^- \rangle$ to $\langle \pi^- \rangle$ ratio for **Ar+Sc** shows a monotonic rise with increasing collision energy.
  Weak dependence on system size.
- No clear system size dependence of $\langle K^+ \rangle$ to $\langle K^- \rangle$ ratio. Monotonic decrease with collision energy.

More results on the subject will follow in the near future!

Thank you for your attention!

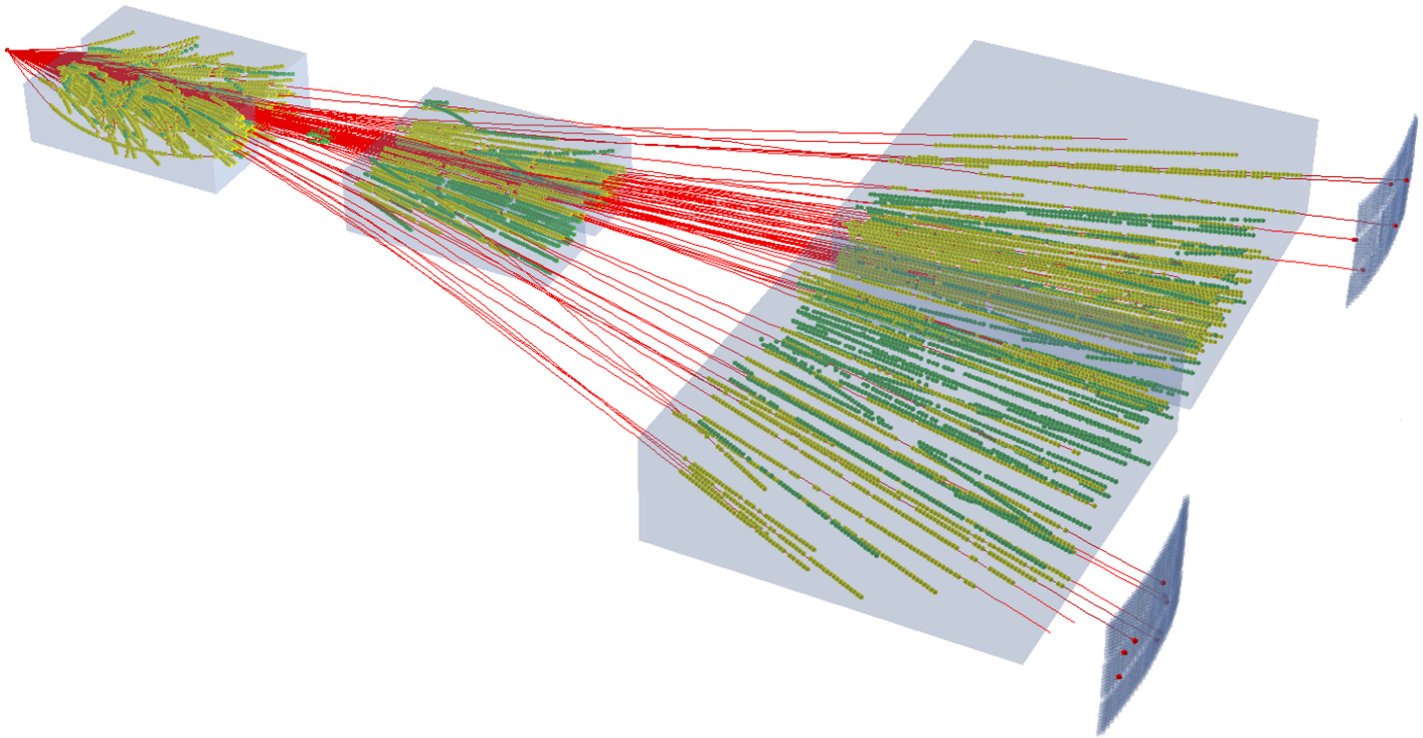

Event of Ar+Sc collision
as recorded by NA61/SHINE

Backup slides

Centrality selection in Ar+Sc collisions

Projectile Spectator Detector

Due to the:

- Ratio of *Fermi motion* to the beam rapidity,
- Differences in magnetic field and
- PSD position for various energies,

different set of modules is chosen to calculate the E_F:

13 *A*GeV/c

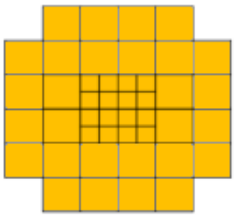

19 *A*GeV/c

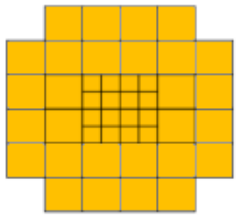

30 *A*GeV/c

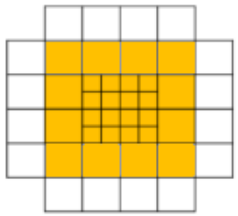

40 *A*GeV/c

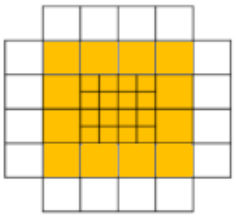

75 *A*GeV/c

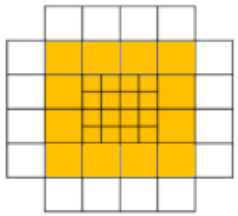

150 *A*GeV/c

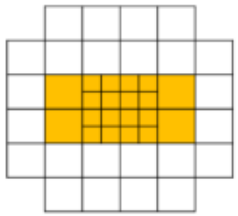

The module sets are chosen on the basis of corelations between energy and multiplicity for each module.